A NONITERATIVE RECONSTRUCTION METHOD FOR SOLVING A TIME-FRACTIONAL INVERSE SOURCE PROBLEM FROM PARTIAL BOUNDARY MEASUREMENTS

R. PRAKASH, M. HRIZI, AND A.A. NOVOTNY

Abstract. In this paper, a noniterative method for solving an inverse source problem governed by the two-dimensional time-fractional diffusion equation is proposed. The basic idea consists in reconstructing the geometrical support of the unknown source from partial boundary measurements of the associated potential. A Kohn-Vogelius type shape functional is considered together with a regularization term penalizing the relative perimeter of the unknown set of anomalies. Identifiability result is derived and uniqueness of a minimizer is ensured. The shape functional measuring the misfit between the solutions of two auxiliary problems containing information about the boundary measurements is minimized with respect to a finite number of ball-shaped trial anomalies by using the topological derivative method. In particular, the second-order topological gradient is exploited to devise an efficient and fast noniterative reconstruction algorithm. Finally, some numerical experiments are presented, showing different features of the proposed approach in reconstructing multiple anomalies of varying shapes and sizes by taking noisy data into account.

1. Introduction

Inverse problems of time-fractional differential equations have attracted great attention from many researchers, particularly in recent years because of their role in many practical domains, which are used in modeling several phenomena in different areas of science such as biology [21, 43], chemistry [62, 63], mechanics [39, 47], physics [64], economy [46], environment [65], and control theory [41]. See also [42] and references therein.

In this paper, we analyze an inverse source problem governed by the two-dimensional time-fractional diffusion equation of order $\alpha \in (0, 1)$. The aim is to reconstruct the spatial component (with an unknown support) present in the source term of a time-fractional diffusion equation from the knowledge of partial boundary measurements. This kind of inverse problems arises, for example, in anomalous diffusion phenomena in heterogeneous media. More precise and detailed information concerning this problem can be found in [48].

There are several works treating the reconstruction of the spatial component in the source term of a time-fractional diffusion equation from an internal observation data, or final overdetermining data, or total/partial boundary measurements. Sakamoto and Yamamoto discussed in [49] an inverse problem of determining a spatially varying function of the source by final overdetermining data, while Wang et al., in [55], used a reproducing kernel space method to solve an inverse space-dependent source problem from the final observation data. Then, Wei and Wang, in [57, 58], proposed a modified quasi-boundary value method for identifying the space-dependent source term with the help of final observation data. Wang et al., in [54], used the Tikhonov regularization method and a simplified Tikhonov regularization method to solve the inverse space-dependent

2020 *Mathematics Subject Classification.* 49N45, 35R11, 35Q93, 35C20, 49M15.

Key words and phrases. Inverse source problem, time-fractional diffusion equation, Kohn-Vogelius formulation, topological derivative method.

problem and established the convergence estimates. The unique recovery of the space-dependent source by interior observation was proved in [29, 30] using Duhamel's principle and unique continuation principle, which also gave an iterative reconstruction algorithm. In [66], Zhang and Xu proposed a numerical method to determine the space-dependent source term from the Cauchy data at one end of a one-dimensional domain. More recently, in [48], Rundell and Zhang determined a source which is supported in a geometrical domain from external boundary measurements. On the other hand, the classical parabolic case (i.e. $\alpha = 1$) has been studied by many authors [20, 22, 26]. Similar inverse problems arise from many important applications and have received considerable recent attention. The reconstruction of the time-dependent source term or coefficient in the time-fractional diffusion equation is one such problem, see for instance [12, 37, 50, 56, 59, 61].

In most of the works mentioned above, the proposed reconstruction approaches are based on iterative algorithms. In the present paper, we address the problem of multiples anomalies reconstruction from partial boundary measurements with the help of a noniterative method. The proposed approach is based on the Kohn-Vogelius formulation and the topological derivative method [44]. More precisely, we aim to reconstruct an unknown space-dependent source term which is supported in $\omega^* \subset \Omega$, where $\Omega \subset \mathbb{R}^2$ with boundary $\partial\Omega$, from a partial boundary measurement of the associated potential on the boundary $\Sigma \subset \partial\Omega$. In order to overcome the ill-posedness, the considered inverse problem is reformulated as a self-regularized topology optimization one where the mass distribution is the unknown variable. The considered misfit function contains two main terms. The first one is defined by a Kohn-Vogelius type functional measuring the misfit between the solutions of two auxiliary problems containing information about the boundary measurements. The second one involves a regularization term penalizing the relative perimeter of the unknown domains. To reconstruct the location, size, shape and number of the mass density distributions in the geometrical domain Ω, an asymptotic expansion of the Kohn-Vogelius functional with respect to a finite number of ball-shaped trial anomalies is computed using the topological derivative method. The second-order topological gradient is exploited to develop an efficient and fast noniterative reconstruction algorithm.

The rest of this paper is organized as follows. Section 2 states the inverse source problem. In Section 3, the considered inverse problem is rewritten in the form of a topology optimization one, which consists of minimizing a Kohn-Vogelius type functional with respect to a set of ball-shaped anomalies. While in Section 4, we present some theoretical results concerning uniqueness of the inverse problem and the considered optimization problem. Then, in Section 5, we derive a second-order asymptotic expansion of a Kohn-Vogelius type functional with respect to a finite number of circular anomalies. The resulting reconstruction method is presented in Section 6, together with the associated reconstruction algorithm. In Section 7, we present numerical examples that demonstrate the effectiveness of the devised reconstruction algorithm. Finally, the paper ends with some concluding remarks in Section 8.

2. Problem statement

Let Ω be an open bounded domain in $\mathbb{R}^2$ with sufficiently smooth boundary $\partial\Omega$. We assume that the diffusion process in Ω is governed by the following time-fractional boundary value problem

$$\left\{\begin{array}{rcll} \partial_t^\alpha u - \Delta u + u &=& F^* & \text{in} \quad \Omega \times (0,T), \\ u &=& 0 & \text{on} \quad \partial\Omega \times (0,T), \\ u(.,0) &=& 0 & \text{in} \quad \Omega, \end{array}\right. \tag{2.1}$$

where u represents the concentration for the diffusion process, $T > 0$ is a given fixed final time, and ∂_t^α denotes the Caputo fractional left derivative of order $0 < \alpha < 1$ with respect

to t and is defined by (see, e.g., [33, p.91])

$$\partial_t^\alpha u(x,t) := \frac{1}{\Gamma(1-\alpha)} \int_0^t (t-\tau)^{-\alpha} \frac{\partial u}{\partial \tau}(x,\tau) \mathrm{d}\tau, \tag{2.2}$$

where Γ denotes Euler's Gamma function, which is defined on each complex number $z \in \mathbb{C}$ with positive real part (i.e. $\Re\{z\} > 0$), by

$$\Gamma(z) = \int_0^\infty s^{z-1} e^{-s} \mathrm{d}s. \tag{2.3}$$

The Caputo derivative is of use to modeling phenomena which takes account of interactions within the past and also problems with non-local properties. In this sense, one can think of the equation as having "memory". Generally, from a physical view-point the fractional diffusion equation is obtained from a fractional Fick law which describes transport processes with long memory, see, e.g., [19] and the references therein. Particularly, in the current paper, the model (2.1) represents a so-called anomalous diffusion process generalizing classical, Brownian diffusion based on the heat equation (see, e.g., [48]).

Note that if α tends to 1, the fractional derivative ∂_t^α tends to the classical first-order derivative $\partial_t u$, and thus the corresponding solution u of the model (2.1) converges to the solution of a parabolic diffusion equation [24, p. 68].

In this work, we assume that the source term F^*, in the governing equation (2.1), is unknown and must be reconstructed from a partial measurement of boundary data. It is well known that the boundary measurement is insufficient to uniquely determine a general source F^* (see, e.g., [31, Section 1.3.1]), and additional assumptions have to be imposed in order to restore unique recovery. To overcome this difficulty, in this work, we assume that the source term F^* receives contribution from space and time variables in a decomposed format. More precisely, we aim to determine an unknown source of the form

$$F^*(x,t) = f^*(x)\mu(t), \tag{2.4}$$

where f^* is a space-dependent source magnitude function whereas μ denotes the attenuation factor with time in the diffusion phenomena.

Keeping the above points in mind, in this article, we are interested in studying the following inverse source problem.

Inverse problem. Let μ be a given non-null function in $C^1([0,T])$ satisfying $\mu(0) \neq 0$ and $\Sigma \subset \partial\Omega$ be an arbitrary open subset of $\partial\Omega$ with non zero measure. Assume that the spatial component f^* is supported in an unknown sub-domain $\omega^* \subset \Omega$; i.e. $f^* = \chi_{\omega^*}$ where χ_{ω^*} is the characteristic function of ω^*. The inverse problem, we investigate in this paper, is about determining the location and shape of the spatial component $f^* = \chi_{\omega^*}$ from the additional inversion input data

$$\varphi(x,t) = \partial_\nu u(x,t), \quad (x,t) \in \Sigma \times (0,T), \tag{2.5}$$

where ν is the outward unit normal vector to $\partial\Omega$.

Remark 1. *The boundary data φ for which this problem has a solution f^* are said to be compatible.*

To address this inverse problem, in the current article, we develop an alternative approach based on the Kohn-Vogelius formulation and the second-order topological derivative concept.

3. Optimization problem

In this section, we exploit the Kohn-Vogelius formulation and formulate our inverse source problem as an optimization one. To this end, we first introduce the set of the

admissible sources terms. It contains the characteristic functions having the form

$$\mathcal{A}(\Omega) = \{\chi_\omega : \Omega \mapsto \mathbb{R} \mid \omega \subset \Omega \text{ is a Lebesgue measurable set}\}. \tag{3.1}$$

The Kohn-Vogelius formulation rephrases the inverse problem into a topological optimization one. In fact, this formulation leads to define two auxiliary problems for any given admissible space-dependent source $\chi_\omega \in \mathcal{A}(\Omega)$.

- The first one is called the "Dirichlet problem": Find $u_D(\omega)$, such that

$$\begin{cases} \partial_t^\alpha u_D(\omega) - \Delta u_D(\omega) + u_D(\omega) &= \chi_\omega\, \mu \quad \text{in} \quad \Omega \times (0,T), \\ u_D(\omega) &= 0 \quad \text{on} \quad \partial\Omega \times (0,T), \\ u_D(\omega)(.,0) &= 0 \quad \text{in} \quad \Omega. \end{cases} \tag{3.2}$$

- The second one is called the "Neumann problem": Find $u_N(\omega)$, such that

$$\begin{cases} \partial_t^\alpha u_N(\omega) - \Delta u_N(\omega) + u_N(\omega) &= \chi_\omega\, \mu \quad \text{in} \quad \Omega \times (0,T), \\ u_N(\omega) &= 0 \quad \text{on} \quad (\partial\Omega \setminus \overline{\Sigma}) \times (0,T), \\ \partial_\nu u_N(\omega) &= \varphi \quad \text{on} \quad \Sigma \times (0,T), \\ u_N(\omega)(.,0) &= 0 \quad \text{in} \quad \Omega. \end{cases} \tag{3.3}$$

These problems assume that the medium is big enough so that the potential decays to zero on the portion of the boundary that is not measured ($\partial\Omega \setminus \overline{\Sigma}$). The solution to (2.1), due to the uniqueness of the traces of $u_D(\omega)$ and $u_N(\omega)$ on $\Sigma \times (0,T)$, is:

$$\text{If } \chi_\omega = \chi_{\omega^*} \Rightarrow u_D(\omega) = u_N(\omega), \tag{3.4}$$

where ω^* is spacial support of unknown source which is the solution of inverse problem, we are dealing with. According to this observation, we find the solution by formulating the inverse problem as a topology optimization problem which minimizes the so-called Kohn–Vogelius functional in the set of admissible sources (3.1):

$$\underset{\chi_\omega \in \mathcal{A}(\Omega)}{\text{Minimize}}\ J_\rho(\chi_\omega), \tag{3.5}$$

where the shape functional $J_\rho(\chi_\omega)$ is defined as

$$J_\rho(\chi_\omega) := \mathcal{J}(u_D(\omega), u_N(\omega)) = \int_0^T \Big(\int_\Omega |\nabla(u_D(\omega) - u_N(\omega))|^2 \mathrm{d}x \Big) \mathrm{d}t + \rho \mathrm{Per}(\omega). \tag{3.6}$$

Moreover, $\rho > 0$ is a regularization parameter and $\mathrm{Per}(\omega)$ denotes the relative perimeter of ω in Ω which is defined as

$$\mathrm{Per}(\omega) = \sup \Big\{ \int_\omega \mathrm{div}\ \phi \ \Big|\ \phi \in C_c^1(\Omega)^2,\ |\phi(x)|_\infty \le 1,\ x \in \Omega \Big\}, \tag{3.7}$$

with $|\cdot|_\infty$ denotes the ℓ_∞-norm in $\mathbb{R}^2$, defined by $|x|_\infty = \max_{1 \le j \le 2} |x_j|$ and $C_c^1(\Omega)$ is the space of continuously differentiable functions with compact support in Ω. Furthermore, if $\mathrm{Per}(\omega) < \infty$, we say that ω has finite perimeter in the domain Ω. In this case, the relative perimeter of ω coincides with the total variation of the distributional gradient of the characteristic function of ω, namely: $\mathrm{Per}(\omega) = |\nabla \chi_\omega|(\Omega)$.

For the sake of completeness of this section, let us briefly browse the history of this kind of cost function. Its main idea was introduced in 1985 by Wexler et al. [60] where a procedure to detect the unknown impedance from boundary measurements was proposed. While, in 1987, Kohn and Vogelius [35] suggested a modification in Wexler's procedure to present it as an alternating choice by proposing a new misfit gap-cost functional. In 1990, this formulation was first used for the numerical implementation of inverse conductivity problems by Kohn and Mackenney [34] and then generalized to several other inverse problems [1, 9, 10, 25].

4. Mathematical analysis

This section is concerned with a mathematical analysis of the considered inverse problem. We will present two main theoretical results. The first one is devoted to the identifiability issue related to the inverse problem. The second one is concerned with the existence and uniqueness of an optimal solution of the optimization problem (3.5). We start our analysis by introducing some definitions as well as some useful results.

4.1. **Notations and preliminary results.** Let $AC([0,T])$ be the space of functions v which are absolutely continuous on $[0,T]$. For $1 \leq p < \infty$, let $L^p(\Omega)$, $H_0^1(\Omega)$, $H^1(\Omega)$, and $H^2(\Omega)$ be the usual classical Lebesgue and Sobolev spaces. By $H^\alpha(0,T)$ we mean the fractional Sobolev space on the interval $(0,\, T)$ (see Adams [2, Chapter VII]). For the solution regularity of problems (3.2) and (3.3), we define the fractional Sobolev spaces ${}_0H^\alpha(0,T)$ as

$${}_0H^\alpha(0,T) = \begin{cases} H^\alpha(0,T), & \text{if } 0 < \alpha < 1/2, \\ \Big\{ g \in H^{1/2}(0,T) : \displaystyle\int_0^T \frac{|g(t)|^2}{t} \mathrm{d}t < \infty \Big\}, & \text{if } \alpha = 1/2, \\ \Big\{ g \in H^\alpha(0,T) : \ g(0) = 0 \Big\}, & \text{if } 1/2 < \alpha < 1. \end{cases}$$

In a Banach space Y, we denote the weak convergence of a sequence $\{X_n\}_{n\geq 1}$ to X by

$$X_n \rightharpoonup X \ \text{ in } \ Y \ \text{ as } n \to \infty.$$

Now, we need some auxiliary results, which will be used in the sequel.

Definition 2. *(see* [33]*). Let $g \in L^2(0,T)$, then for $\alpha > 0$ the Riemann-Liouville integral operator I_{0+}^α and the backward Riemann-Liouville integral operator I_{T-}^α are defined by*

$$I_{0+}^\alpha g(t) = \frac{1}{\Gamma(\alpha)} \int_0^t (t-\tau)^{\alpha-1} g(\tau) \mathrm{d}\tau, \quad 0 < t \leq T, \tag{4.1}$$

and

$$I_{T-}^\alpha g(t) = \frac{1}{\Gamma(\alpha)} \int_t^T (t-\tau)^{\alpha-1} g(\tau) \mathrm{d}\tau, \quad 0 < t \leq T. \tag{4.2}$$

Moreover, the Caputo derivative ∂_t^α can be rewritten as

$$\partial_t^\alpha g(t) = I_{0+}^{1-\alpha} g'(t), \quad 0 < t \leq T. \tag{4.3}$$

Lemma 3. *Let $g \in L^2(0,T)$, for $\alpha, \gamma > 0$ we have*

$$(I_{0+}^\alpha o\, I_{0+}^\gamma) g(t) = (I_{0+}^\gamma o\, I_{0+}^\alpha) g(t) = I_{0+}^{\alpha+\gamma} g(t). \tag{4.4}$$

Proof. See Lemma 1.3(iv) in [36]. □

On the basis of [49, Theorem 2.1(i)] and [17, Proposition 5.2], we give the unique continuation result as follows:

Lemma 4. *For given $a(x) \in L^2(\Omega)$ and Σ is a nonempty part of $\partial\Omega$, let v be the solution to the following fractional diffusion equation with the homogeneous Dirichlet boundary condition:*

$$\begin{cases} \partial_t^\alpha v(x,t) - \Delta v(x,t) + v(x,t) &= 0, & (x,t) \in \Omega \times (0,T), \\ v(x,t) &= 0, & (x,t) \in \partial\Omega \times (0,T), \\ v(x,0) &= a(x), & x \in \Omega. \end{cases} \tag{4.5}$$

Then problem (4.5) *admits a unique solution $v \in C\left([0,T]; L^2(\Omega)\right) \cap C\left((0,T]; H^2(\Omega) \cap H_0^1(\Omega)\right)$. Moreover,*

$$\partial_\nu v = 0 \ \text{ on } \Sigma \times (0,T) \quad \text{ implies } \quad v = 0 \ \text{ in } \Omega \times (0,T).$$

Lemma 5. *(Duhamel's principle). Let $F(x,t) = f(x)\kappa(t)$, where $f \in L^2(\Omega)$ and $\kappa \in C^1[0,T]$. Let ψ be the solution to the fractional diffusion equation*

$$\begin{cases} \partial_t^\alpha \psi(x,t) - \Delta\psi(x,t) + \psi(x,t) &= F(x,t), \quad (x,t) \in \Omega \times (0,T), \\ \psi(x,t) &= 0, \qquad (x,t) \in \partial\Omega \times (0,T), \\ \psi(x,0) &= 0, \qquad x \in \Omega. \end{cases} \tag{4.6}$$

Then the weak solution ψ of the problem (4.6) can be represented as

$$\psi(\cdot,t) = \int_0^t \theta(t-s)\vartheta(\cdot,s)\mathrm{d}s, \quad 0 < t < T,$$

where ϑ solves the homogeneous problem

$$\begin{cases} \partial_t^\alpha \vartheta(x,t) - \Delta\vartheta(x,t) + \vartheta(x,t) &= 0, \qquad (x,t) \in \Omega \times (0,T), \\ \vartheta(x,t) &= 0, \qquad (x,t) \in \partial\Omega \times (0,T), \\ \vartheta(x,0) &= f(x), \quad x \in \Omega, \end{cases} \tag{4.7}$$

and $\theta \in L^1(0,T)$ is the unique solution to the fractional integral equation

$$I_{0+}^{1-\alpha}\theta(t) = \kappa(t), \quad 0 < t < T.$$

Proof. See [38, Lemma 4.1]. □

Lemma 6. *(Alikhanov inequality). For any function $v(t) \in AC([0,T])$, one has the inequality*

$$\frac{1}{2}\partial_t^\alpha v^2(t) \le v(t)\partial_t^\alpha v(t), \quad 0 < \alpha < 1.$$

Proof. The proof of this lemma can be found in [4, Lemma 1]. □

The well-posedness of the boundary value problems (3.2) and (3.3) are provided by the following result.

Lemma 7. *Let $f \in L^2(\Omega)$ be a spatial component in the source term of the time-fractional diffusion problems (3.2) and (3.3). Then,*

(1) *the Dirichlet problem (3.2) has a unique weak solution $u_D \in {}_0H^\alpha(0,T;L^2(\Omega)) \cap L^2(0,T;H^2(\Omega) \cap H_0^1(\Omega)) \cap C([0,T];L^2(\Omega))$. Moreover, there exists a constant $c > 0$ depending on Ω, T, α, and μ such that*

$$\|u_D\|_{H^\alpha(0,T;L^2(\Omega))} + \|u_D\|_{L^2(0,T;H^2(\Omega))} \le c\|f\|_{L^2(\Omega)}. \tag{4.8}$$

(2) *for given $\varphi \in L^2(0,T;L^2(\Sigma))$, the Neumanne problem (3.3) has a unique weak solution $u_N \in L^2(0,T;H^1(\Omega)) \cap {}_0H^\alpha(0,T;L^2(\Omega))$. Moreover, there exist some constants $c, C > 0$ such that*

$$\partial_t^\alpha \|u_N\|_{L^2(\Omega)}^2 + c\|u_N\|_{H^1(\Omega)}^2 \le C\Big[\|f\|_{L^2(\Omega)}^2 + \|\varphi\|_{L^2(\Sigma)}^2\Big]. \tag{4.9}$$

Proof. Based on [29, Lemma 2.4] and [49, Theorem 2.2(i)], we can obtain the existence and uniqueness of a weak solutions of the Dirichlet problem (4.5).

Following the result of [32, Theorem 2.4], the Neumann problem (3.3) admits a unique weak solution. Now, we prove the estimation (4.9).

By taking u_N as a test function in the weak formulation of the Neumann problem (3.3), we deduce

$$\int_\Omega (\partial_t^\alpha u_N)u_N\mathrm{d}x + \int_\Omega \Big(|\nabla u_N|^2 + |u_N|^2\Big)\mathrm{d}x = \int_\Omega \mu\, f\, u_N\mathrm{d}x + \int_\Sigma \varphi\, u_N\mathrm{d}s. \tag{4.10}$$

Using Cauchy-Schwarz inequality and Trace theorem, we have

$$\begin{aligned}
&\Big|\int_\Omega \mu\, f\, u_N \mathrm{d}x + \int_\Sigma \varphi\, u_N \mathrm{d}s\Big| \\
&\le c\Big(\int_\Omega |f|^2\mathrm{d}x\Big)^{1/2}\Big(\int_\Omega |u_N|^2\mathrm{d}x\Big)^{1/2} + \Big(\int_\Sigma |\varphi|^2\mathrm{d}s\Big)^{1/2}\Big(\int_\Sigma |u_N|^2\mathrm{d}s\Big)^{1/2} \\
&\le c\Big[\Big(\int_\Omega |f|^2\mathrm{d}x\Big)^{1/2}\Big(\int_\Omega |u_N|^2\mathrm{d}x\Big)^{1/2} + \Big(\int_\Sigma |\varphi|^2\mathrm{d}s\Big)^{1/2}\Big(\int_{\partial\Omega} |u_N|^2\mathrm{d}s\Big)^{1/2}\Big] \\
&\le c\Big[\Big(\int_\Omega |f|^2\mathrm{d}x\Big)^{1/2}\Big(\int_\Omega |u_N|^2\mathrm{d}x\Big)^{1/2} + \Big(\int_\Sigma |\varphi|^2\mathrm{d}s\Big)^{1/2}\Big(\int_\Omega (|u_N|^2 + |\nabla u_N|^2)\mathrm{d}x\Big)^{1/2}\Big].
\end{aligned} \tag{4.11}$$

In other hand, the Young inequality implies

$$\begin{aligned}
&\Big(\int_\Omega |f|^2\mathrm{d}x\Big)^{1/2}\Big(\int_\Omega |u_N|^2\mathrm{d}x\Big)^{1/2} + \Big(\int_\Sigma |\varphi|^2\mathrm{d}s\Big)^{1/2}\Big(\int_\Omega (|u_N|^2 + |\nabla u_N|^2)\mathrm{d}x\Big)^{1/2} \\
&\le \gamma_1 \int_\Omega |u_N|^2\mathrm{d}x + \gamma_2 \int_\Omega (|u_N|^2 + |\nabla u_N|^2)\mathrm{d}x + C_1 \int_\Omega |f|^2\mathrm{d}x + C_2 \int_\Sigma |\varphi|^2\mathrm{d}s \\
&\le \gamma \int_\Omega (|\nabla u_N|^2 + |u_N|^2)\mathrm{d}x + C\Big[\int_\Omega |f|^2\mathrm{d}x + \int_\Sigma |\varphi|^2\mathrm{d}s\Big].
\end{aligned} \tag{4.12}$$

Now, we define ${}_0C^1([0,T]) = \{v \in C^1([0,T]);\quad v(0) = 0\}$. Then, from Lemma 2.2 in Kubica et al. [36], we see that $\overline{{}_0C^1([0,T])}^{{}_0H^\alpha(0,T)} = {}_0H^\alpha(0,T)$, hence we can choose u_n in ${}_0C^1[0,T]$ such that

$$u_n \longrightarrow u_N \ \text{ strongly in } H^\alpha(0,T) \ \text{ as } \ n \longrightarrow +\infty.$$

Note that ${}_0C^1([0,T]) \subset AC([0,T])$. So, by applying the Alikhanov inequality (see Lemma 6), we obtain

$$\frac{1}{2}\partial_t^\alpha u_n^2(t) \le (\partial_t^\alpha u_n(t))u_n(t). \tag{4.13}$$

Since $u_n \longrightarrow u_N$ in $H^\alpha(0,T)$, we have $u_n(t) \longrightarrow u_N(t)$ for almost all $t \in (0,T)$. Hence, we get

$$(\partial_t^\alpha u_n(t))u_n(t) \longrightarrow (\partial_t^\alpha u_N(t))u_N(t) \ \text{ for almost all } \ t \in (0,T). \tag{4.14}$$

Now, from relation (4.3) and Lemma 3 and the above convergence result, we obtain

$$I_{0+}^\alpha \partial_t^\alpha u_n^2(t) = u_n^2(t) \longrightarrow u_N^2(t) = I_{0+}^\alpha \partial_t^\alpha u_N^2(t) \ \text{ for almost all } \ t \in (0,T). \tag{4.15}$$

Consequently, we see that

$$\partial_t^\alpha u_n^2(t) \longrightarrow \partial_t^\alpha u_N^2(t) \ \text{ for almost all } \ t \in (0,T). \tag{4.16}$$

By passing the limit $n \longrightarrow \infty$ in (4.13), from (4.14) and (4.16), we get

$$\frac{1}{2}\partial_t^\alpha u_N^2(t) \le (\partial_t^\alpha u_N(t))u_N(t). \tag{4.17}$$

Thus,

$$\frac{1}{2}\partial_t^\alpha \|u_N\|_{L^2(\Omega)}^2 \le \int_\Omega (\partial_t^\alpha u_N)u_N \mathrm{d}x. \tag{4.18}$$

Finally inserting (4.11)-(4.12) and (4.18) in (4.10), we obtain the desired result. This completes the proof. □

We provide the following lemmas which will be used in the proof of the existence of an optimal solution to the optimization problem (3.5).

Lemma 8. *(see* [29, Lemma 4.1]*). For* $0 < \alpha < 1$ *and* $\theta_1, \theta_2 \in L^2(0,T)$*, it holds*

$$\int_0^T \Big(I_{0+}^{\alpha}\theta_1(t)\Big)\theta_2(t)\,\mathrm{d}t = \int_0^T \theta_1(t)\Big(I_{T-}^{\alpha}\theta_2(t)\Big)\,\mathrm{d}t. \tag{4.19}$$

Lemma 9. *(see* [3, Lemma 4]*). Let* $\theta \in {}_0H^{\alpha}(0,T) \cap C([0,T])$ *and* $g \in C^1([0,T])$*. Then*

$$\int_0^T \Big(\partial_t^{\alpha}\theta\Big)g\,\mathrm{d}t = \theta(T)I_{T-}^{1-\alpha}g(T) - \theta(0)I_{T-}^{1-\alpha}g(0) - \int_0^T \theta\Big(I_{T-}^{1-\alpha}g\Big)'\,\mathrm{d}t. \tag{4.20}$$

Lemma 10. *(see* [13, Theorem 6.3 in Chapter 5]*). Let* $\{\mathcal{O}_n\}_n$ *be a sequence of measurable domains in* Ω *for which there exists a constant* $c > 0$ *such that*

$$\forall n, \quad \mathrm{Per}\,(\mathcal{O}_n) \le c.$$

Then there exist a measurable set $\mathcal{O}^*$ *in* Ω *and a subsequence* $\{\mathcal{O}_{n_k}\}_k$ *such that*

$$\chi_{\mathcal{O}_{n_k}} \to \chi_{\mathcal{O}^*} \text{ in } L^1(\Omega) \text{ as } k \to \infty, \tag{4.21}$$

and

$$\mathrm{Per}(\mathcal{O}^*) \le \liminf_{k\to\infty} \mathrm{Per}\,(\mathcal{O}_{n_k}) \le c. \tag{4.22}$$

4.2. **Identifiability.** In this section, we discuss the identifiability question related to the considered inverse source problem. It is concerned to the well-posedness of the optimization problem. We prove that the source $f^* = \chi_{\omega^*}$ is uniquely determined from a partial boundary measurement data φ on $\Sigma \times (0,T)$. The established result is summarized in the following theorem. The prove of this result follows similar arguments as appeared in [29].

Theorem 11. *For a given* $\mu \in C^1([0,T])$ *with* $\mu(0) \neq 0$ *and* $\Sigma \subset \partial\Omega$ *an arbitrarily open domain, let* $f_i^* = \chi_{\omega_i^*} \in \mathcal{A}(\Omega)$*,* $i = \{1,2\}$ *such that the solutions* u_i *of the boundary value problem*

$$\begin{cases} \partial_t^{\alpha}u_i(x,t) - \Delta u_i(x,t) + u_i(x,t) &= f_i^*(x)\mu(t), & (x,t) \in \Omega \times (0,T), \\ u_i(x,t) &= 0, & (x,t) \in \partial\Omega \times (0,T), \\ u_i(x,0) &= 0, & x \in \Omega, \end{cases} \tag{4.23}$$

satisfy

$$\partial_\nu u_1 = \partial_\nu u_2 = \varphi \quad \text{on } \Sigma \times (0,T); \tag{4.24}$$

then $f_1^* = f_2^* = f^*$*; i.e* $\omega_1^* = \omega_2^* = \omega^*$*.*

Proof. Consider the difference $W_{2,1} := u_2 - u_1$, which is the solution to

$$\begin{cases} \partial_t^{\alpha}W_{2,1}(x,t) - \Delta W_{2,1}(x,t) + W_{2,1}(x,t) &= (f_2^*(x) - f_1^*(x))\mu(t), & (x,t) \in \Omega \times (0,T), \\ W_{2,1}(x,t) &= 0, & (x,t) \in \partial\Omega \times (0,T), \\ W_{2,1}(x,0) &= 0, & x \in \Omega. \end{cases}$$

From Lemma 5, $W_{2,1}$ has the representation

$$W_{2,1}(x,t) = \int_0^t \theta(t-\tau)\vartheta(x,\tau)\mathrm{d}\tau, \quad (x,t) \in \Omega \times (0,T), \tag{4.25}$$

where ϑ solves the homogeneous problem

$$\begin{cases} \partial_t^{\alpha}\vartheta(x,t) - \Delta\vartheta(x,t) + \vartheta(x,t) &= 0, & (x,t) \in \Omega \times (0,T), \\ \vartheta(x,t) &= 0, & (x,t) \in \partial\Omega \times (0,T), \\ \vartheta(x,0) &= f_2^*(x) - f_1^*(x), & x \in \Omega, \end{cases} \tag{4.26}$$

and $\theta(t) \in L^1(0,T)$ is the unique solution to the fractional integral equation

$$I_{0+}^{1-\alpha}\theta(t) = \mu(t), \quad 0 < t < T. \tag{4.27}$$

Differentiating two sides of equality (4.25) with respect to $x \in \Sigma \subset \partial\Omega$, we obtain

$$\partial_\nu W_{2,1}(x,t) = \int_0^t \theta(t-\tau)\partial_\nu \vartheta(x,\tau)\mathrm{d}\tau, \quad (x,t) \in \Sigma \times (0,T). \tag{4.28}$$

If we apply the Riemann-Liouville integral operator to (4.28) and change the order of the integrations, we obtain

$$\begin{aligned} I_{0+}^{1-\alpha}\partial_\nu W_{2,1}(x,t) &= \frac{1}{\Gamma(1-\alpha)}\int_0^t \frac{1}{(t-\tau)^\alpha}\int_0^\tau \theta(\tau-\xi)\partial_\nu\vartheta(x,\xi)\mathrm{d}\xi\mathrm{d}\tau \\ &= \frac{1}{\Gamma(1-\alpha)}\int_0^t \partial_\nu\vartheta(x,\xi)\int_\xi^t \frac{\theta(\tau-\xi)}{(t-\tau)^\alpha}\mathrm{d}\tau\mathrm{d}\xi \\ &= \int_0^t \partial_\nu\vartheta(x,\xi)\Big[\frac{1}{\Gamma(1-\alpha)}\int_0^{t-\xi}\frac{\theta(\tau)}{(t-\xi-\tau)^\alpha}\mathrm{d}\tau\Big]\mathrm{d}\xi. \end{aligned}$$

In other hand, from (4.1) and (4.27), we deduce that

$$\begin{aligned} I_{0+}^{1-\alpha}\partial_\nu W_{2,1}(x,t) &= \int_0^t \partial_\nu\vartheta(x,\xi) I_{0+}^{1-\alpha}\theta(t-\xi)\mathrm{d}\xi \\ &= \int_0^t \mu(t-s)\partial_\nu\vartheta(x,s)\mathrm{d}s. \end{aligned}$$

Moreover, according to (4.24), we have $\partial_\nu W_{2,1} = \partial_\nu u_2 - \partial_\nu u_1 = 0$ on $\Sigma \times (0,T)$. Consequently,

$$\int_0^t \mu(t-s)\partial_\nu\vartheta(x,s)\mathrm{d}s = 0, \quad x \in \Sigma.$$

We deduce that,

$$0 = \frac{\mathrm{d}}{\mathrm{d}t}\Big(\int_0^t \mu(t-s)\partial_\nu\vartheta(x,s)\mathrm{d}s\Big) = \mu(0)\partial_\nu\vartheta(x,t) + \int_0^t \mu'(t-s)\partial_\nu\vartheta(x,s)\mathrm{d}s \quad \text{on} \quad \Sigma\times(0,T).$$

Owing to the assumption that $\mu(0) \neq 0$, the following estimate holds true for $0 < t < T$

$$\begin{aligned} \|\partial_\nu\vartheta(.,t)\|_{L^2(\Sigma)} &\leq \frac{1}{|\mu(0)|}\int_0^t |\mu'(t-s)|\,\|\partial_\nu\vartheta(\cdot,s)\|_{L^2(\Sigma)}\,\mathrm{d}s \\ &\leq \frac{\|\mu\|_{C^1([0,T])}}{|\mu(0)|}\int_0^t \|\partial_\nu\vartheta(\cdot,s)\|_{L^2(\Sigma)}\,\mathrm{d}s. \end{aligned}$$

Then, by the Gronwall's inequality, $\partial_\nu\vartheta$ is identically null on $\Sigma \times (0,T)$. Hence, thanks to Lemma 4, we know that $\vartheta = 0$ in $\Omega \times (0,T)$, which implies $f_2^* - f_1^* = 0$ in Ω (i.e. $\omega_1^* = \omega_2^*$). The proof is complete. □

4.3. **Uniqueness of a minimizer.** The aim of introducing the regularization term in (3.6) is relevant for the existence of the optimal solution of the considered optimization problem, which is discussed in the following theorem.

Theorem 12. *For any $\rho > 0$ there exists a unique solution $\chi_{\omega^*} \in \mathcal{A}(\Omega)$ of the minimization problem (3.5), i.e.*

$$J_\rho(\chi_{\omega^*}) \leq J_\rho(\chi_\omega) \quad \textit{for all } \chi_\omega \in \mathcal{A}(\Omega). \tag{4.29}$$

Proof. The functional J_ρ is bounded below by zero and hence, there exists a minimizing decreasing sequence $\{\chi_{\omega_n}\}_n \subset \mathcal{A}(\Omega)$ such that

$$\lim_{n\to\infty} J_\rho(\chi_{\omega_n}) = \inf_{\chi_\omega \in \mathcal{A}(\Omega)} J_\rho(\chi_\omega).$$

W.l.o.g, we assume that $J_\rho(\chi_{\omega_0}) < \infty$. As

$$\rho\,\mathrm{Per}(\omega_n) \leq J_\rho(\chi_{\omega_n}) \leq J_\rho(\chi_{\omega_0}) \quad \text{for all } n \in \mathbb{N}.$$

Consequently, we have

$$\mathrm{Per}\,(\omega_n) \leq \frac{J_\rho\,(\chi_{\omega_0})}{\rho} \quad \text{for all } n \in \mathbb{N}.$$

Therefore, in view of Lemma 10, there exist a measurable set $\omega^* \subset \Omega$ and a subsequence of $\{\chi_{\omega_n}\}_{n\geq 1}$, still denoted by $\{\chi_{\omega_n}\}_{n\geq 1}$, such that

$$\chi_{\omega_n} \longrightarrow \chi_{\omega^*} \text{ in } L^1(\Omega) \text{ as } n \longrightarrow \infty. \tag{4.30}$$

We prove that χ_{ω^*} is indeed the unique minimizer to (3.5). For each $n \in \mathbb{N}$, let $u_D(\omega_n)$ and $u_N(\omega_n)$ be solutions of the problems (3.2) and (3.3) with $\omega = \omega_n$, (i.e. $\chi_\omega = \chi_{\omega_n}$), respectively. Next, we examine the convergence of the Dirichlet solution $u_D(\omega_n)$. The convergence of $u_N(\omega_n)$ follows analogically.

From Lemma 7, we can deduce that the sequence $\{u_D(\omega_n)\}_{n\geq 1}$ is bounded in ${}_0H^\alpha(0,T;L^2(\Omega)) \cap L^2(0,T;H^2(\Omega)\cap H_0^1(\Omega))$. This ensures the existence of some u_D^* in ${}_0H^\alpha(0,T;L^2(\Omega)) \cap L^2(0,T;H^2(\Omega)\cap H_0^1(\Omega))$ and a subsequence of $\{u_D(\omega_n)\}_{n\geq 1}$, still denoted by $\{u_D(\omega_n)\}_{n\geq 1}$ such that

$$u_D(\omega_n) \rightharpoonup u_D^* \text{ in } {}_0H^\alpha(0,T;L^2(\Omega)) \cap L^2(0,T;H^2(\Omega)\cap H_0^1(\Omega)) \text{ as } n \longrightarrow \infty. \tag{4.31}$$

In the next step, we aim to show that

$$u_D^* = u_D(\omega^*).$$

The variational formulation of (3.2) with $\omega = \omega_n$ implies

$$\int_0^T \int_\Omega \Big(\partial_t^\alpha u_D(\omega_n) v + \nabla u_D(\omega_n)\cdot\nabla v + u_D(\omega_n) v\Big)\mathrm{d}x\mathrm{d}t = \int_0^T \int_\Omega \chi_{\omega_n}\,\mu\, v\;\mathrm{d}x\mathrm{d}t, \tag{4.32}$$

for all $v \in L^2(0,T;H_0^1(\Omega))$. Due to (4.31), it follows

$$\partial_t^\alpha u_D(\omega_n) \rightharpoonup \partial_t^\alpha u_D^*, \quad \nabla u_D(\omega_n) \rightharpoonup \nabla u_D^* \text{ in } L^2(\Omega\times(0,T)) \text{ as } n \longrightarrow \infty. \tag{4.33}$$

Tending n to infinity, from (4.32) one can obtain

$$\int_0^T \int_\Omega \Big(\partial_t^\alpha u_D^* v + \nabla u_D^*\cdot\nabla v + u_D^* v\Big)\;\mathrm{d}x\mathrm{d}t = \int_0^T \int_\Omega \chi_{\omega^*}\,\mu\, v\;\mathrm{d}x\mathrm{d}t, \tag{4.34}$$

for all $v \in L^2(0,T;H_0^1(\Omega))$. Next, we shall prove $u_D^*(.,0) = 0$, which with (4.34) and the definition of weak solutions of (3.2) implies $u_D^* = u_D(\omega^*)$.

Using Lemma 7, we have $u_D(\omega_n) \in {}_0H^\alpha(0,T;L^2(\Omega)) \cap C([0,T];L^2(\Omega))$ which satisfies the assumption of Lemma 9. Therefore, by taking $\varphi \in C^1([0,T])$ with $I_{T-}^{1-\alpha}\varphi(T) = 0$ and using Lemma 9, we obtain

$$\int_0^T \Big(\partial_t^\alpha u_D(\omega_n)\Big)\varphi\;\mathrm{d}t = -u_D(\omega_n)(.,0) I_{T-}^{1-\alpha}\varphi(0) - \int_0^T u_D(\omega_n)\Big(I_{T-}^{1-\alpha}\varphi\Big)'\;\mathrm{d}t. \tag{4.35}$$

Let $\theta \in L^2(\Omega)$ arbitrary. By multiplying the above equation with θ, then, integrating it in space and using the fact that $u_D(\omega_n)(.,0) = 0$ in Ω, we have

$$\int_\Omega \int_0^T \Big(\partial_t^\alpha u_D(\omega_n)\Big)\varphi\theta\;\mathrm{d}t\mathrm{d}x = -\int_\Omega \int_0^T u_D(\omega_n)\Big(I_{T-}^{1-\alpha}\varphi\Big)'\theta\;\mathrm{d}t\mathrm{d}x. \tag{4.36}$$

If n tends to infinity, from (4.31), one can obtain

$$\int_\Omega \int_0^T \Big(\partial_t^\alpha u_D^*\Big)\varphi\theta\;\mathrm{d}t\mathrm{d}x = -\int_\Omega \int_0^T u_D^*\Big(I_{T-}^{1-\alpha}\varphi\Big)'\theta\;\mathrm{d}t\mathrm{d}x. \tag{4.37}$$

On other hand, we have

$$\int_\Omega \int_0^T \Big(\partial_t^\alpha u_D^*\Big)\varphi\theta \,\mathrm{d}t\mathrm{d}x = -\int_\Omega u_D^*(.,0)\Big(I_{T-}^{1-\alpha}\varphi(0)\Big)\theta \,\mathrm{d}x - \int_\Omega \int_0^T u_D^*\Big(I_{T-}^{1-\alpha}\varphi\Big)'\theta \,\mathrm{d}t\mathrm{d}x, \tag{4.38}$$

for any $\varphi \in C^1([0,T])$ with $I_{T-}^{1-\alpha}\varphi(T) = 0$ and $\theta \in L^2(\Omega)$.
Combining (4.35) and (4.38), we obtain

$$\int_\Omega u_D^*(.,0)\Big(I_{T-}^{1-\alpha}\varphi(0)\Big)\theta \,\mathrm{d}x = 0, \;\; \forall \theta \in L^2(\Omega). \tag{4.39}$$

Hence,

$$u_D^*(.,0) = 0. \tag{4.40}$$

Then one can conclude that

$$u_D^* = u_D(\omega^*). \tag{4.41}$$

By the same way, we can prove the existence of some $u_N^* \in {}_0H^\alpha(0,T;L^2(\Omega)) \cap L^2(0,T;H^1(\Omega))$ and a subsequence of $\{u_N(\omega_n)\}_{n\geq 1}$, still denoted by $\{u_N(\omega_n)\}_{n\geq 1}$ such that

$$u_N(\omega_n) \rightharpoonup u_N^* \text{ in } {}_0H^\alpha(0,T;L^2(\Omega)) \cap L^2(0,T;H^1(\Omega)) \text{ as } n \longrightarrow \infty. \tag{4.42}$$

Moreover, we have

$$u_N^* = u_N(\omega^*).$$

The last part of this proof is due to the lower semi-continuity of the cost function J_ρ. Indeed, it is well known that the $L^2(\Omega)$-norm is lower semi-continuous. The lower semi-continuity of the second term in J_ρ (the perimeter function) follows from Lemma 10-(4.22). Then, combining the lower semi-continuity of J_ρ with the convergence results (4.30), (4.31) and (4.42), one can deduce

$$J_\rho(\chi_{\omega^*}) \leq \liminf_{n\to\infty} J_\rho(\chi_{\omega_n}) \leq J_\rho(\chi_\omega), \;\; \forall \chi_\omega \in \mathcal{A}(\Omega),$$

indicating that χ_{ω^*} is indeed a minimizer to the optimization problem (3.5). Moreover, the uniqueness of χ_{ω^*} is readily seen from strict convexity of $J_\rho(\chi_\omega)$. Thus the proof of the Theorem is complete. □

Since the considered inverse problem has been rewritten as a topology optimization problem (3.5), we seek to solve it by using the topological derivative method, which is described in Section 5. In the rest of the paper, to simplify notation, we denote $u_D(\omega)$ and $u_N(\omega)$ by u_D and u_N for the initial guess ω, respectively.

5. Sensitivity analysis

The topological derivative measures the sensitivity of a given shape function with respect to a small singular topological perturbation, such as the insertion of cavities, inclusions, source-terms or even cracks. The topological derivative was introduced in the field of shape optimization by Schumacher et al. [51, 14] and was for the first time mathematically justified in [18, 52]. Since then, this concept has been successfully applied to solve many relevant problems such as inverse problems, topology optimization, image processing, multi-scale constitutive modeling, fracture and damage mechanics, and many other applications [45].

In this paper, we derive a second-order topological asymptotic expansion for the considered shape function $\mathcal{J}$ from (3.6) with respect to the presence of a finite number of ball-shaped anomalies. To this end, we need to introduce some notations and useful assumptions. Let $n \geq 1$ be a given integer. For each $1 \leq i \leq n$, we denote by $\mathcal{B}_{\varepsilon_i}(z_i)$ the

ball of radius ε_i and center at $z_i \in \Omega$. We assume that the balls $\mathcal{B}_{\varepsilon_i}(z_i)$ are disjoints and strictly included inside the domain Ω; i.e.

$$\overline{\mathcal{B}_{\varepsilon_i}(z_i)} \subset \Omega \text{ such that } \mathcal{B}_{\varepsilon_i}(z_i) \cap \mathcal{B}_{\varepsilon_j}(z_j) = \emptyset,\ \forall i, j \in \{1, ..., n\} \text{ and } i \neq j.$$

It is well known that the energy-like misfit function from (3.6) without the regularization term $\mathrm{Per}(\omega)$ (i.e. $\rho = 0$) have repeatedly been noticed to be self-regularizing (see, for instance, [5, 11]), which means they don't need an additional regularization to stabilize the reconstruction process. Therefore, the aim of introducing the regularization term is to prove (only) the well-posedness of the optimization problem (3.5). Hence, for the sake of simplicity, we assume that $\mathrm{Per}(\omega) < \infty$ and we take $\rho = |\varepsilon|^5$ where $\varepsilon = (\varepsilon_1, \cdots, \varepsilon_n)$ and $|\varepsilon| = \varepsilon_1 + \cdots + \varepsilon_n$. Thus, $\rho\,\mathrm{Per}(\omega) = o(|\varepsilon|^4)$. In addition, we know that the source term of the time-fractional diffusion problems (3.2) and (3.3) is given by

$$F(x,t) = \chi_\omega(x)\,\mu(t).$$

Since $\mu(t)$ is given, then the perturbed counterpart of the source term F can be defined as

$$F_\varepsilon(x,t) = F(x,t) + \sum_{i=1}^{n} \rho_i \chi_{\mathcal{B}_{\varepsilon_i}(z_i)}, \tag{5.1}$$

where $\rho_i \in \mathbb{R}^+$ is related to the mean value of $\mu(t)$ over the ball $\mathcal{B}_{\varepsilon_i}(z_i)$, $i = 1, \cdots, n$. Therefore, the Kohn-Vogelius functional associated with the perturbed source term F_ε is written as

$$\mathcal{J}(u_D^\varepsilon, u_N^\varepsilon) := \int_0^T \Big(\int_\Omega |\nabla(u_D^\varepsilon - u_N^\varepsilon)|^2 \mathrm{d}x \Big) \mathrm{d}t + o(|\varepsilon|^4), \tag{5.2}$$

where u_D^ε and u_N^ε are solutions of

$$\left\{ \begin{array}{rcccc} \partial_t^\alpha u_D^\varepsilon - \Delta u_D^\varepsilon + u_D^\varepsilon &=& F_\varepsilon & \text{in} & \Omega \times (0,T), \\ u_D^\varepsilon &=& 0 & \text{on} & \partial\Omega \times (0,T), \\ u_D^\varepsilon(.,0) &=& 0 & \text{in} & \Omega, \end{array} \right. \tag{5.3}$$

$$\left\{ \begin{array}{rcccc} \partial_t^\alpha u_N^\varepsilon - \Delta u_N^\varepsilon + u_N^\varepsilon &=& F_\varepsilon & \text{in} & \Omega \times (0,T), \\ u_N^\varepsilon &=& 0 & \text{on} & (\partial\Omega \backslash \overline{\Sigma}) \times (0,T), \\ \partial_\nu u_N^\varepsilon &=& \varphi & \text{on} & \Sigma \times (0,T), \\ u_N^\varepsilon(.,0) &=& 0 & \text{in} & \Omega. \end{array} \right. \tag{5.4}$$

The following sections are concerned with the variation of $\mathcal{J}$ with respect to the presence of the anomalies $\mathcal{B}_{\varepsilon_i}(z_i)$ in the domain Ω. In order to provide an asymptotic expansion of the Kohn-Vogelius functional $\mathcal{J}$, we need first an asymptotic expansion of some modified Bessel functions.

5.1. **Series expansions for Bessel functions.** We denote the modified Bessel functions of the first kind and order m by I_m, with $m \in \mathbb{Z}$. As $x \to 0^+$, we have the following asymptotic expansions:

$$I_0(x) = 1 + \frac{1}{4}x^2 + O(x^4), \tag{5.5}$$

and

$$I_1(x) = \frac{1}{2}x + \frac{1}{16}x^3 + O(x^5). \tag{5.6}$$

The modified Bessel functions of the second kind and order m are denoted by K_m, with $m \in \mathbb{Z}$. As $x \to 0^+$, we have the following asymptotic expansions:

$$K_0(x) = (\ln 2 - \mathrm{e}) - \ln x - \frac{1}{4}x^2 \ln x + \frac{1}{4}(1 + \ln 2 - \mathrm{e})x^2 + O(x^4), \tag{5.7}$$

and

$$K_1(x) = \frac{1}{x} + \frac{1}{2}x\ln x + \frac{1}{2}(\mathrm{e} - \ln 2 - \frac{1}{2})x + \frac{1}{16}x^3\ln x + \frac{1}{16}(\mathrm{e} - \ln 2 - \frac{5}{4})x^3 + O(x^5), \quad (5.8)$$

where e is the Euler constant. The above series expansions are obtained from Jeffrey et al. [28].

5.2. **Asymptotic analysis of the solutions.** Let us introduce the following ansätze for the solutions to the perturbed problems (5.3) and (5.4):

$$u_D^{\varepsilon}(x,t) = u_D(x,t) + \sum_{i=1}^{n} \rho_i \pi \varepsilon_i^2 v_D^{\varepsilon_i}(x), \quad (5.9)$$

$$u_N^{\varepsilon}(x,t) = u_N(x,t) + \sum_{i=1}^{n} \rho_i \pi \varepsilon_i^2 v_N^{\varepsilon_i}(x), \quad (5.10)$$

where u_D and u_N are the solutions of the Dirichlet (3.2) and Neumann (3.3) problems. In addition, $v_D^{\varepsilon_i}$ and $v_N^{\varepsilon_i}$ are the solutions of the following auxiliary boundary value problems for $i = 1, \cdots, n$:

$$\left\{ \begin{array}{rcll} -\Delta v_D^{\varepsilon_i} + v_D^{\varepsilon_i} &=& \frac{1}{\pi\varepsilon_i^2}\chi_{\mathcal{B}_{\varepsilon_i}(z_i)} & \text{in} \quad \Omega, \\ v_D^{\varepsilon_i} &=& 0 & \text{on} \quad \partial\Omega, \end{array} \right. \quad (5.11)$$

and

$$\left\{ \begin{array}{rcll} -\Delta v_N^{\varepsilon_i} + v_N^{\varepsilon_i} &=& \frac{1}{\pi\varepsilon_i^2}\chi_{\mathcal{B}_{\varepsilon_i}(z_i)} & \text{in} \quad \Omega, \\ v_N^{\varepsilon_i} &=& 0 & \text{on} \quad \partial\Omega\backslash\overline{\Sigma}, \\ \partial_\nu v_N^{\varepsilon_i} &=& 0 & \text{on} \quad \Sigma. \end{array} \right. \quad (5.12)$$

Since $v_D^{\varepsilon_i}$ and $v_N^{\varepsilon_i}$ depend on ε_i in the ball $\mathcal{B}_{\varepsilon_i}(z_i)$, let us separate them into two parts:

$$v_D^{\varepsilon_i}(x) = p^{\varepsilon_i}(x) + \lambda_3^{\varepsilon_i} q_D^i(x), \quad (5.13)$$

$$v_N^{\varepsilon_i}(x) = p^{\varepsilon_i}(x) + \lambda_3^{\varepsilon_i} q_N^i(x), \quad (5.14)$$

where p^{ε_i} is solution of the following boundary value problem defined in a big ball $\mathcal{B}_R(z_i) \supset \Omega$ of radius R and centre at z_i:

$$\left\{ \begin{array}{rcll} -\Delta p^{\varepsilon_i} + p^{\varepsilon_i} &=& \frac{1}{\pi\varepsilon_i^2}\chi_{\mathcal{B}_{\varepsilon_i}(z_i)} & \text{in} \quad \mathcal{B}_R(z_i), \\ p^{\varepsilon_i} &=& \lambda_3^{\varepsilon_i} K_0(R) & \text{on} \quad \partial\mathcal{B}_R(z_i). \end{array} \right. \quad (5.15)$$

The above boundary value problem admits the explicit solution of the form

$$p^{\varepsilon_i}(x) = \left\{ \begin{array}{ll} \lambda_1^{\varepsilon_i} - \lambda_2^{\varepsilon_i} I_0(|x - z_i|), & x \in \mathcal{B}_{\varepsilon_i}(z_i), \\ \lambda_3^{\varepsilon_i} K_0(|x - z_i|), & x \in \mathcal{B}_R(z_i) \setminus \overline{\mathcal{B}_{\varepsilon_i}(z_i)}, \end{array} \right. \quad (5.16)$$

where

$$\lambda_1^{\varepsilon_i} = \frac{1}{\pi\varepsilon_i^2}, \quad (5.17)$$

$$\lambda_2^{\varepsilon_i} = \frac{1}{\pi\varepsilon_i^2} \frac{K_1(\varepsilon_i)}{K_0(\varepsilon_i)I_1(\varepsilon_i) + K_1(\varepsilon_i)I_0(\varepsilon_i)}, \quad (5.18)$$

and

$$\lambda_3^{\varepsilon_i} = \frac{1}{\pi\varepsilon_i^2} \frac{I_1(\varepsilon_i)}{K_0(\varepsilon_i)I_1(\varepsilon_i) + K_1(\varepsilon_i)I_0(\varepsilon_i)}. \quad (5.19)$$

We can use the asymptotic expansions (5.5)-(5.8) to rewrite (5.18) and (5.19) as follows:

$$\lambda_2^{\varepsilon_i} = \frac{1}{\pi\varepsilon_i^2} + \lambda_0 + \frac{1}{2\pi}\ln\varepsilon_i + O(\varepsilon_i^2), \quad (5.20)$$

and

$$\lambda_3^{\varepsilon_i} = \frac{1}{2\pi} + \frac{1}{16\pi}\varepsilon_i^2 + O(\varepsilon_i^4), \quad (5.21)$$

with

$$\lambda_0 = \frac{1}{4\pi}(2\mathrm{e} - 2\ln 2 - 1). \tag{5.22}$$

Finally, $\lambda_3^{\varepsilon_i} q_D^i$ and $\lambda_3^{\varepsilon_i} q_N^i$ must compensate for the discrepancies left by p^{ε_i} on $\partial\Omega$. In particular, they are the solutions to the following boundary value problems:

$$\left\{ \begin{array}{rcll} -\Delta q_D^i + q_D^i &=& 0 & \text{in} \quad \Omega, \\ q_D^i &=& -K_0(|x - z_i|) & \text{on} \quad \partial\Omega, \end{array} \right. \tag{5.23}$$

$$\left\{ \begin{array}{rcll} -\Delta q_N^i + q_N^i &=& 0 & \text{in} \quad \Omega, \\ q_N^i &=& -K_0(|x - z_i|) & \text{on} \quad \partial\Omega\backslash\overline{\Sigma}, \\ \partial_\nu q_N^i &=& -\partial_\nu K_0(|x - z_i|) & \text{on} \quad \Sigma. \end{array} \right. \tag{5.24}$$

Consequently, from (5.9)-(5.10), (5.13)-(5.14), and (5.21), the difference between u_D^ε and u_N^ε is simply given by

$$u_D^\varepsilon - u_N^\varepsilon = u_D - u_N + \sum_{i=1}^{n} \rho_i \varepsilon_i^2 \Big(\frac{1}{2} + \frac{1}{16}\varepsilon_i^2 \Big) h_i + o(|\varepsilon|^4), \tag{5.25}$$

with $h_i = q_D^i - q_N^i$.

5.3. **Asymptotic analysis of the Kohn-Vogelius functional.** By replacing expansion (5.25) in the definition of the perturbed counterpart of the shape functional (5.2) and then collecting terms with the same power of ε_i and ε_j, we obtain the following topological asymptotic expansion

$$\begin{aligned} \mathcal{J}(u_D^\varepsilon, u_N^\varepsilon) - \mathcal{J}(u_D, u_N) &= \sum_{i=1}^{n} \rho_i \varepsilon_i^2 \int_\Omega \nabla h_i \cdot \left(\int_0^T \nabla(u_D - u_N) \mathrm{d}t \right) \mathrm{d}x \\ &+ \frac{1}{8} \sum_{i=1}^{n} \rho_i \varepsilon_i^4 \int_\Omega \nabla h_i \cdot \left(\int_0^T \nabla(u_D - u_N) \mathrm{d}t \right) \mathrm{d}x \\ &+ \frac{T}{4} \sum_{i,j=1}^{n} \rho_i \rho_j \varepsilon_i^2 \varepsilon_j^2 \int_\Omega \nabla h_i \cdot \nabla h_j \, \mathrm{d}x + o(|\varepsilon|^4), \end{aligned} \tag{5.26}$$

where $\mathcal{J}(u_D, u_N)$ is the original unperturbed shape function given by (3.6).

6. Reconstruction algorithm

In this section, we want to find a better approximation to the target ω^* than the initial guess ω based on the topological asymptotic expansion of the Kohn-Vogelius shape functional given by (5.26). Therefore, let us introduce the following quantity

$$\Psi(\beta, \zeta) = \beta \cdot d(\zeta) + \frac{1}{2} H(\zeta)\beta \cdot \beta, \tag{6.1}$$

where vectors $\zeta = (z_1, \cdots, z_n)$ and $\beta = (\beta_1, \cdots \beta_n)$, with $\beta_i = \rho_i \varepsilon_i^2$, so that n is the number of anomalies to be reconstructed, ζ are their locations and β their sizes. Finally, vector d and matrix H have entries

$$d(\zeta) = \begin{pmatrix} d_1 \\ d_2 \\ \vdots \\ d_n \end{pmatrix} \quad \text{and} \quad H(\zeta) = \begin{pmatrix} H_{11} & H_{12} & \cdots & H_{1n} \\ H_{21} & H_{22} & \cdots & H_{2n} \\ \vdots & \vdots & \ddots & \vdots \\ H_{n1} & H_{n2} & \cdots & H_{nn} \end{pmatrix}, \tag{6.2}$$

where

$$d_i = \int_\Omega \nabla h_i \cdot \left(\int_0^T \nabla(u_D - u_N) \mathrm{d}t \right) \mathrm{d}x, \tag{6.3}$$

$$H_{ii} = \frac{1}{4\rho_i} \int_\Omega \nabla h_i \cdot \left(\int_0^T \nabla(u_D - u_N) \mathrm{d}t \right) \mathrm{d}x + \frac{T}{2} \int_\Omega \nabla h_i \cdot \nabla h_i \, \mathrm{d}x, \tag{6.4}$$

$$H_{ij} = \frac{T}{2} \int_\Omega \nabla h_i \cdot \nabla h_j \, \mathrm{d}x \quad \text{for} \quad i \neq j. \tag{6.5}$$

Given the function (6.1), its minimum is trivially found when

$$\langle D_\beta \Psi(\beta, \zeta), \delta\beta \rangle = 0, \quad \forall \delta\beta \in \mathbb{R}^n. \tag{6.6}$$

Since H_{ij} is symmetric positive definite, the minimization of the function $\Psi(\beta, \zeta)$ with respect to β leads to the global minimum. In particular,

$$(H(\zeta)\beta + d(\zeta)) \cdot \delta\beta = 0, \quad \forall \, \delta\beta \in \mathbb{R}^n \quad \Rightarrow \quad H(\zeta)\beta = -d(\zeta), \tag{6.7}$$

provided that $H = H^\top$. Therefore,

$$\beta = \beta(\zeta) = -H(\zeta)^{-1} d(\zeta), \tag{6.8}$$

such that the quantity β, solving (6.8), becomes a function of the locations ζ. After replacing the solution of (6.8) into $\Psi(\beta, \zeta)$, defined by (6.1), the optimal locations $\zeta^\star$ can be obtained from a combinatorial search over the domain Ω. These locations are the solutions to the following minimization problem:

$$\zeta^\star = \underset{\zeta \in Z}{\operatorname{argmin}} \left\{ \Psi(\beta(\zeta), \zeta) = \frac{1}{2} \beta(\zeta) \cdot d(\zeta) \right\}, \tag{6.9}$$

where Z is the set of admissible locations of anomalies. Problem (6.9) is solved by a combinatorial search over the set of admissible locations Z. Since this step is bottleneck of the proposed approach, we refer to [40] for more sophisticated strategies based on meta-heuristic and multigrid schemes for solving the minimization problem (6.9). Then, the optimal sources are characterized by the pair $\zeta^\star$ and $\beta^\star = \beta(\zeta^\star)$ of locations and sizes, respectively.

To summarize, we have introduced a second order topology optimization algorithm which is able to find the optimal sizes $\beta^\star$ of the hidden anomalies and their locations $\zeta^\star$ for a given number n of trial balls. The inputs to the algorithm are:

- the vector d and the matrix H;
- the $m = \mathrm{card}(Z)$ points at which the system (6.8) is solved;
- the number n of anomalies to be reconstructed.

The algorithm returns the optimal sizes $\beta^\star$ and locations $\zeta^\star$. The above procedure is written in pseudo-code format as shown in Algorithm 1. In the algorithm, Π maps the vector of nodal indices $\mathcal{I} = (i_1, i_2, \ldots, i_n)$ to the corresponding vector of nodal coordinates ζ. For further applications of this algorithm, we refer to [9, 15, 16], which can be combined with well-established and more computationally sophisticated iterative methods [6, 7, 23, 27, 53].

7. Numerical results

Let us consider a circular domain $\Omega = \{x \in \mathbb{R}^2 : |x| < 1\}$, with unit radius and centre at the origin. The boundary value problems are discretized by using standard Finite Element Method in space and Finite Difference Method in time following the same procedure as described in [48]. In particular, the domain Ω is discretized into 524288 three-node finite elements. The set of admissible locations Z is obtained by selecting 49 interior nodes from the finite elements mesh. See sketch in Figure 1, where the points

Algorithm 1: Second Order Reconstruction Algorithm

input : d, H, m, n;
output: the optimal solution $\Psi^\star$, $\beta^\star$, $\zeta^\star$;

Initialization: $\Psi^\star \leftarrow \infty$; $\beta^\star \leftarrow 0$; $\zeta^\star \leftarrow 0$;
for $i_1 \leftarrow 1$ **to** m **do**
  for $i_2 \leftarrow i_1 + 1$ **to** m **do**
    $\vdots$
    for $i_n \leftarrow i_{n-1} + 1$ **to** m **do**
      $$d \leftarrow \begin{bmatrix} d_{(i_1)} \\ d_{(i_2)} \\ \vdots \\ d_{(i_n)} \end{bmatrix}; \quad H \leftarrow \begin{bmatrix} H_{(i_1,i_1)} & H_{(i_1,i_2)} & \cdots & H_{(i_1,i_n)} \\ H_{(i_2,i_1)} & H_{(i_2,i_2)} & \cdots & H_{(i_2,i_n)} \\ \vdots & \vdots & \ddots & \vdots \\ H_{(i_n,i_1)} & H_{(i_n,i_2)} & \cdots & H_{(i_n,i_n)} \end{bmatrix};$$
      $\mathcal{I} \leftarrow (i_1, i_2, \ldots, i_n)$; $\zeta \leftarrow \Pi(\mathcal{I})$; $\beta \leftarrow -H^{-1}d$; $\Psi \leftarrow \frac{1}{2} d \cdot \beta$;
      if $\Psi < \Psi^\star$ **then**
        $\zeta^\star \leftarrow \zeta$; $\beta^\star \leftarrow \beta$; $\Psi^\star \leftarrow \Psi$;
      end if
    end for
  end for
end for
return $\Psi^\star$, $\beta^\star$, $\zeta^\star$;

belonging to Z are represented by black dots. We note that, once the location of the true anomaly does not belong to the set of admissible locations Z, the reconstruction algorithm returns the optimal location closest to the true one. See for instance the original work [8]. Therefore, for the sake of simplicity, we assume that the true locations of anomalies, to be reconstructed, always belongs to the set Z. Finally, the final time is set as $T = 1$ and the resulting interval $(0, 1)$ is discretized into 100 uniform time steps.

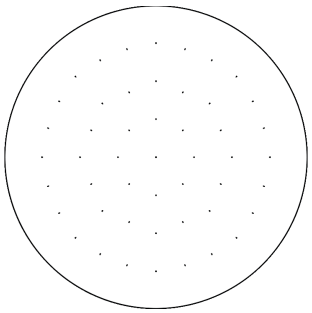

FIGURE 1. Domain Ω and set of admissible locations Z represented by 49 black dots.

The source $F^*(x,t)$ to be reconstructed is given by

$$F^*(x,t) = \sum_{i=1}^{n} \mu_i(t) \chi_{\omega_i^*}(x), \tag{7.1}$$

where n is the number of hidden anomalies ω_i^*, with $\omega_i^* \cap \omega_j^* = \varnothing$, for $i \neq j$. The mean values of functions $\mu_i(t)$ are set as $\bar{\mu}_i = 1$, for $i = 1, \cdots, n$. This choice simplifies the graphical representation of the results since each unknown is defined as $\beta_i = \rho_i \varepsilon_i^2$. That is

to say, it is expected to obtain a value of β_i coinciding with the size of the i-th anomaly. Note that the number of anomalies n to be reconstructed is arbitrary. However, for the sake of simplicity, we assume that n is given. In the case of unknown n, see for instance [8].

In order to verify the robustness of the method with respect to noisy data, the true source term F^* is corrupted with White Gaussian Noise (WGN) of zero mean and standard deviation η. Note that, in this context, noisy data can be interpreted as modeling uncertainties.

In the pictures to be presented in the next sections, the observable boundary Σ is represented by dashed lines, whereas the hidden boundary $\partial\Omega \setminus \overline{\Sigma}$ is depicted as solid lines. Finally, we set $\omega = \varnothing$, which means that all the examples are free of initial guess.

7.1. **Example 1.** In this example, we consider the reconstruction of a cross-shaped anomaly with one trial ball ($n = 1$) from partial boundary measurement. The function $\mu_1(t) = 10\chi_{(0.0,0.1)}$, so that $\bar{\mu}_1 = 1$. The target is corrupted with varying levels of noise, namely $\eta \in \{0, 10, 20, 40, 80\}\%$ as shown in Figure 2, left column. The obtained results by setting α close to zero ($\alpha = 0.0001$) as well as α close to one ($\alpha = 0.9999$) are presented in Figure 2, middle and right columns, respectively. From an analysis of these figures, we observe that the centre of the trial ball coincides with the barycentre of the cross-shaped anomaly and the resulting volumes are very close to each other, up to $\eta = 40\%$. In the case of $\alpha = 0.0001$, the reconstructed volume is slice underestimated. For $\eta = 80\%$, the result is degraded. It shows that a trial ball can be used to approximate the cross-shaped anomaly even in the presence of high level of noise. Note that the behaviour of the reconstruction algorithm is quite similar for both values of α, so that in the next examples, we fix $\alpha = 0.5$.

7.2. **Example 2.** Now, let us consider the simultaneous reconstruction of two identical circular-shaped anomalies with two trial balls ($n = 2$) from pointwise boundary measurement. In particular, the observable boundary Σ is now given by four points uniformly distributed on $\partial\Omega$. The functions $\mu_1(t) = 10\chi_{(0.0,0.1)}$ and $\mu_2(t) = 5\chi_{(0.2,0.4)}$, so that $\bar{\mu}_1 = \bar{\mu}_2 = 1$. The target to be reconstructed and the obtained result for $\alpha = 0.5$ are presented in Figure 3. In this case, the target is successfully reconstructed even from a small amount of information given by four points of observation.

7.3. **Example 3.** In this example, we consider the simultaneous reconstruction of two circular-shaped anomalies with two trial balls ($n = 2$) from partial boundary measurement. Now, one anomaly is much bigger than the other one. The functions $\mu_1(t) = 10\chi_{(0.0,0.1)}$ and $\mu_2(t) = 5\chi_{(0.2,0.4)}$, which gives $\bar{\mu}_1 = \bar{\mu}_2 = 1$. The target to be reconstructed and the obtained result for $\alpha = 0.5$ are presented in Figure 4. From an analysis of the figure, we observe that there is a small discrepancy on the size of the smaller ball, whose reconstructed radius is underestimated. However, the reconstruction can be considered satisfactory.

7.4. **Example 4.** Now, let us consider the simultaneous reconstruction of three identical circular-shaped anomalies with three trial balls ($n = 3$) from partial boundary measurement. The functions $\mu_1(t) = 10\chi_{(0.0,0.1)}$, $\mu_2(t) = 5\chi_{(0.2,0.4)}$ and $\mu_3(t) = 2.5\chi_{(0.3,0.7)}$, so that $\bar{\mu}_1 = \bar{\mu}_2 = \bar{\mu}_3 = 1$. Two configurations for the observable boundary are taken into account, Σ_1 and Σ_2, such that Σ_1 is bigger than Σ_2. The target to be reconstructed for $\alpha = 0.5$ is presented in Figure 5, left. The obtained results for Σ_1 and Σ_2 are presented in Figure 5, middle and right, respectively. From an analysis of these figures, we observe that the target is perfectly reconstructed for the bigger observable boundary Σ_1. However, the reconstruction fails for the smaller observable boundary Σ_2. Therefore, the amount of

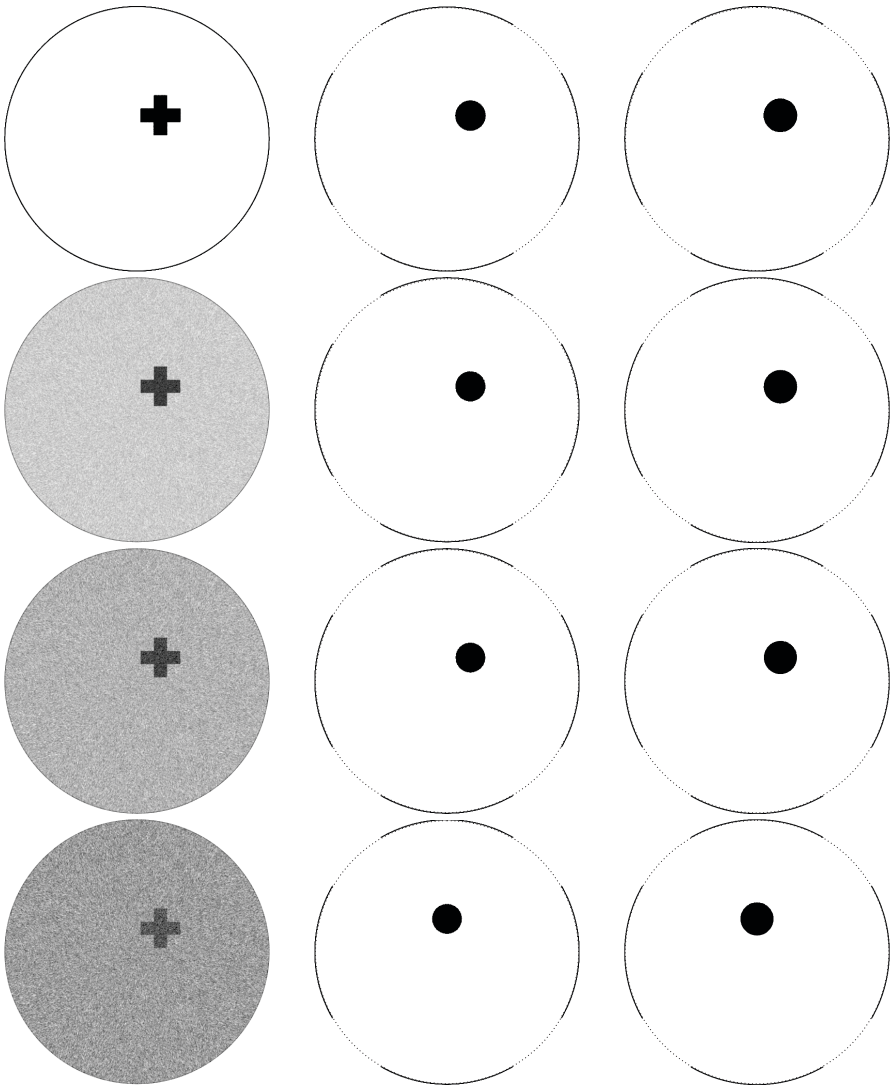

FIGURE 2. Example 1: Target to be reconstructed (left column) and obtained reconstructions with $n = 1$ trial ball for $\alpha = 0.0001$ (middle column) and $\alpha = 0.9999$ (right column). The level of noise is increased from the first to the four line as $\eta \in \{0, 20, 40, 80\}\%$. The dashed and solid lines are used to represent the observable Σ and the hidden $\partial\Omega \setminus \overline{\Sigma}$ boundaries, respectively.

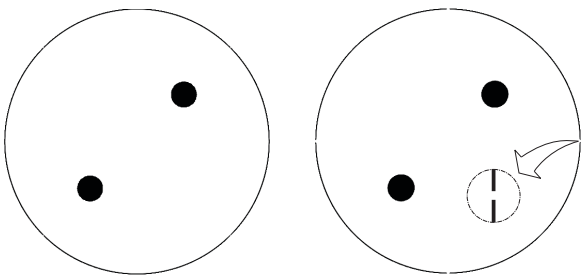

FIGURE 3. Example 2: Target to be reconstructed (left) and obtained reconstruction (right) with $n = 2$ trial balls. See zoom highlighting one of the four points forming the observable boundary Σ.

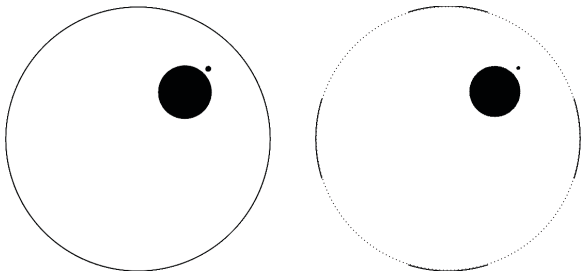

FIGURE 4. Example 3: Target to be reconstructed (left) and obtained reconstruction (right) with $n = 2$ trial balls. The dashed and solid lines are used to represent the observable Σ and the hidden $\partial\Omega \setminus \overline{\Sigma}$ boundaries, respectively.

available information on the boundary affect the reconstruction of complex set of hidden anomalies.

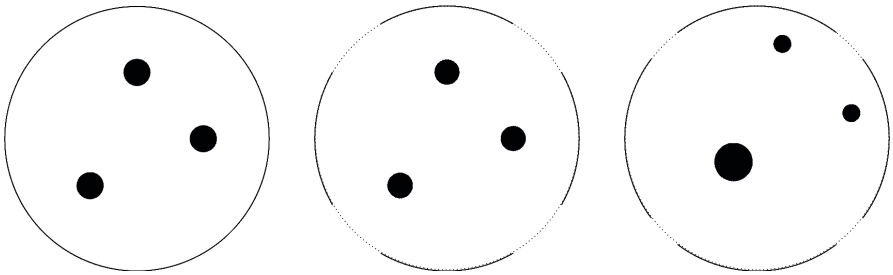

FIGURE 5. Example 4: Target to be reconstructed (left) and obtained reconstructions with $n = 3$ trial balls for the observable boundaries Σ_1 (middle) and Σ_2 (right). The dashed and solid lines are used to represent the observable and the hidden boundaries, respectively.

7.5. **Example 5.** In this example, we consider again the simultaneous reconstruction of three identical circular-shaped anomalies with three trial balls ($n = 3$), but from total boundary measurement. In particular, the observable boundary $\Sigma = \partial\Omega$. The functions $\mu_1(t) = 10\chi_{(0.0,0.1)}$, $\mu_2(t) = 5\chi_{(0.2,0.4)}$ and $\mu_3(t) = 2.5\chi_{(0.3,0.7)}$, thus $\bar{\mu}_1 = \bar{\mu}_2 = \bar{\mu}_3 = 1$. The target is corrupted with varying levels of noise, namely $\eta \in \{10, 20, 30\}\%$ as shown in Figure 6, left column. The obtained results for $\alpha = 0.5$ are presented in Figure 6, right column. From an analysis of these figures, we observe that the target is well reconstructed for $\eta = 10\%$ and $\eta = 20\%$. However, for $\eta = 40\%$ the reconstruction fails.

7.6. **Example 6.** In this last example, we consider the simultaneous reconstruction of two anomalies of different shapes with three trial balls ($n = 3$) from total boundary measurement ($\Sigma = \partial\Omega$). In particular, the first anomaly is circular and the second one is rectangular. The functions $\mu_1(t) = 10\chi_{(0.0,0.1)}$ and $\mu_2(t) = 5\chi_{(0.2,0.4)}$, thus $\bar{\mu}_1 = \bar{\mu}_2$. The target to be reconstructed for $\alpha = 0.5$ and the obtained result are presented in Figure 7, left and right, respectively. From an analysis of this figure, we observe that an arbitrary-shaped target can be approximated by a number of trial balls.

8. Concluding remarks

In this paper, we investigate an inverse source problem for a time-fractional diffusion equation in two spatial dimensions. More precisely, we have tackled the geometric reconstruction of space-dependent source which is supported in an unknown domain from

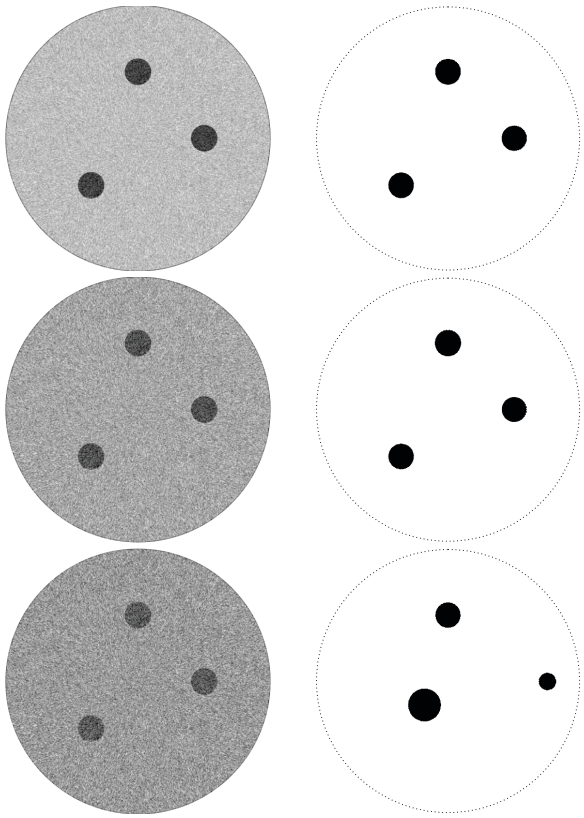

FIGURE 6. Example 5: Target to be reconstructed (left column) and obtained reconstructions with $n = 3$ trial balls (right column). The level of noise is increased from the first to the third line as $\eta \in \{10, 20, 30\}\%$. The dashed line is used to represent the observable boundary $\Sigma = \partial\Omega$.

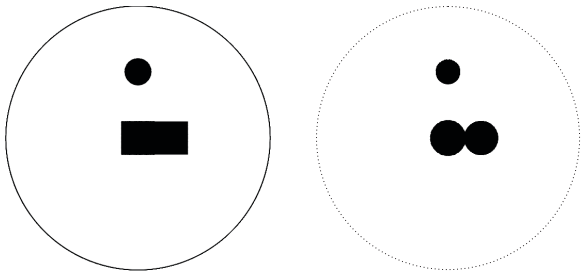

FIGURE 7. Example 6: Target to be reconstructed (left) and obtained reconstruction with $n = 3$ trial balls (right). The dashed line is used to represent the observable boundary $\Sigma = \partial\Omega$.

partial boundary measurements of the potential field. The physical motivation of this problem comes from differences between classical Brownian diffusion and the anomalous case. The general idea of the proposed method consists in rewriting the inverse problem as a self-regularized topology optimization one. The unknown support of the space-dependent source is characterized as the solution to an optimization problem minimizing a given Kohn-Vogelius type functional, with respect to the set of admissible sources, by using the topological derivative method.

The existence and uniqueness for the optimization problem solution and the uniqueness for the inverse problem are both proved. The second-order topological gradient has been used to devise a fast reconstruction algorithm based on a simple optimization step, which

is free of initial guess. Six numerical examples are provided to show that the proposed method is effective and very robust with respect to noisy data.

On the other hand, several mathematical issues of high interest have not been discussed in the paper. The stability problem is one of them. The full stability issue is, however, up to our knowledge, still an open problem which deserves further investigation.

References

[1] A. B. Abda, M. Hassine, M. Jaoua, and M. Masmoudi. Topological sensitivity analysis for the location of small cavities in stokes flow. *SIAM Journal on Control and Optimization*, 48:2871–2900, 2009.

[2] R.A. Adams and J.J.F. Fournier. *Sobolev spaces*. Elsevier, 2003.

[3] M. Ali, S. Aziz, and S. A. Malik. Inverse problem for a space-time fractional diffusion equation: Application of fractional sturm-liouville operator. *Mathematical Methods in the Applied Sciences*, 41(7):2733–2747, 2018.

[4] A. A. Alikhanov. A priori estimates for solutions of boundary value problems for fractional-order equations. *Differential equations*, 46(5):660–666, 2010.

[5] S. Andrieux, T. N. Baranger, and A. B. Abda. Solving cauchy problems by minimizing an energy-like functional. *Inverse Problems*, 22(1):59–65, 2006.

[6] J. Baumeister and A. Leitão. *Topics in inverse problems*. IMPA Mathematical Publications, Rio de Janeiro, 2005.

[7] M. Burger. A level set method for inverse problems. *Inverse Problems*, 17:1327–1356, 2001.

[8] A. Canelas, A. Laurain, and A. A. Novotny. A new reconstruction method for the inverse potential problem. *Journal of Computational Physics*, 268:417–431, 2014.

[9] A. Canelas, A. Laurain, and A. A. Novotny. A new reconstruction method for the inverse source problem from partial boundary measurements. *Inverse Problems*, 31(7):075009, 2015.

[10] F. Caubet and M. Dambrine. Localization of small obstacles in stokes flow. *Inverse Problems*, 28(10):1–31, 2012.

[11] S. Chaabane, C. Elhechmi, and M. Jaoua. A stable recovery method for the robin inverse problem. *Mathematics and Computers in Simulation*, 66(4–5):367–383, 2004.

[12] J. Cheng, J. Nakagawa, M. Yamamoto, and T. Yamazaki. Uniqueness in an inverse problem for a one-dimensional fractional diffusion equation. *Inverse problems*, 25(11):115002, 2009.

[13] M. C. Delfour and J. P. Zolésio. *Shapes and Geometries. Advances in Design and Control*. Society for Industrial and Applied Mathematics (SIAM), Philadelphia, PA, 2001.

[14] H.A. Eschenauer, V.V. Kobelev, and A. Schumacher. Bubble method for topology and shape optmization of structures. *Structural Optimization*, 8(1):42–51, 1994.

[15] L. Fernandez, A. A. Novotny, and R. Prakash. Noniterative reconstruction method for an inverse potential problem modeled by a modified Helmholtz equation. *Numerical Functional Analysis and Optimization*, 39(9):937–966, 2018. DOI: 10.1080/01630563.2018.1432645.

[16] A.D. Ferreira and A. A. Novotny. A new non-iterative reconstruction method for the electrical impedance tomography problem. *Inverse Problems*, 33(3):035005, 2017.

[17] K. Fujishiro. Approximate controllability for fractional diffusion equations by dirichlet boundary control. *arXiv preprint arXiv:1404.0207*, 2014.

[18] S. Garreau, Ph. Guillaume, and M. Masmoudi. The topological asymptotic for PDE systems: the elasticity case. *SIAM Journal on Control and Optimization*, 39(6):1756–1778, 2001.

[19] R. Gorenflo, F. Mainardi, D. Moretti, and P. Paradisi. Time fractional diffusion: a discrete random walk approach. *Nonlinear Dynamics*, 29(1):129–143, 2002.

[20] H. Harbrecht and J. Tausch. An efficient numerical method for a shape-identification problem arising from the heat equation. *Inverse problems*, 27(6):065013, 2011.

[21] B. I. Henry, T. A. M. Langlands, and S. L. Wearne. Fractional cable models for spiny neuronal dendrites. *Physical review letters*, 100(12):128103, 2008.

[22] F. Hettlich and W. Rundell. Identification of a discontinuous source in the heat equation. *Inverse Problems*, 17(5):1465, 2001.

[23] M. Hintermüller and A. Laurain. Electrical impedance tomography: from topology to shape. *Control and Cybernetics*, 37(4):913–933, 2008.

[24] L. Hörmander. *The analysis of linear partial differential operators I. Distribution Theory and Fourier Analysis*. Springer-Verlag, Berlin, 2003.

[25] M. Hrizi and M. Hassine. Reconstruction of contact regions in semiconductor transistors using dirichlet-neumann cost functional approach. *Applicable Analysis*, pages 1–30, 2019. DOI: 10.1080/00036811.2019.1623393.

[26] M. Hrizi, M. Hassine, and R. Malek. A new reconstruction method for a parabolic inverse source problem. *Applicable Analysis*, 2018. DOI: 10.4208/cicp.100710.021210a.

[27] V. Isakov, S. Leung, and J. Qian. A fast local level set method for inverse gravimetry. *Communications in Computational Physics*, 10(4):1044–1070, 2011.

[28] A. Jeffrey and H.H. Dai. *Handbook of mathematical formulas and integrals*. Elsevier, 2008.

[29] D. Jiang, Z. Li, Y. Liu, and M. Yamamoto. Weak unique continuation property and a related inverse source problem for time-fractional diffusion-advection equations. *Inverse Problems*, 33(5):055013, 2017.

[30] D. Jiang, Y. Liu, and D. Wang. Numerical reconstruction of the spatial component in the source term of a time-fractional diffusion equation. *Advances in Computational Mathematics*, 46(:):1–24, 2020.

[31] Y. Kian, E. Soccorsi, Q. Xue, and M. Yamamoto. Identification of time-varying source term in time-fractional diffusion equations. *arXiv preprint arXiv:1911.09951*, 2019.

[32] Y. Kian and M. Yamamoto. Well-posedness for weak and strong solutions of non-homogeneous initial boundary value problems for fractional diffusion equations. *Fractional Calculus and Applied Analysis*, 24:168–201, 2021.

[33] A.A. Kilbas, H.M Srivastava, and J.J. Trujillo. *Theory and applications of fractional differential equations*, volume 204. Elsevier, 2006.

[34] R. Kohn and A. McKenney. Numerical implementation of a variational method for electrical impedance tomography. *Inverse Problems*, 6(3):389, 1990.

[35] R. Kohn and M. Vogelius. Determining conductivity by boundary measurements. *Communications on Pure and Applied Mathematics*, 37(3):289–298, 1984.

[36] A. Kubica, K. Ryszewska, and M. Yamamoto. *Time-fractional Differential Equations: A Theoretical Introduction*. Springer Japan, ToKyo, 2020.

[37] Y.S. Li and T. Wei. An inverse time-dependent source problem for a time-space fractional diffusion equation. *Applied Mathematics and Computation*, 336:257–271, 2018.

[38] Y. Liu, W. Rundell, and M. Yamamoto. Strong maximum principle for fractional diffusion equations and an application to an inverse source problem. *Fractional Calculus and Applied Analysis*, 19(4):888–906, 2016.

[39] L.P. Lociniczak. Analytical studies of a time-fractional porous medium equation: Derivation, approximation and applications. *Communications in Nonlinear Science and Numerical Simulation*, 24(1-3):169–183, 2015.

[40] T. J. Machado, J. S. Angelo, and A. A. Novotny. A new one-shot pointwise source reconstruction method. *Mathematical Methods in the Applied Sciences*, 40(15):1367–1381, 2017.

[41] R. Metzler and J. Klafter. Boundary value problems for fractional diffusion equations. *Physica A: Statistical Mechanics and its Applications*, 278(1–2):107–125, 2000.

[42] R. Metzler and J. Klafter. The random walk's guide to anomalous diffusion: a fractional dynamics approach. *Physics Reports*, 339(1):1–77, 2000.

[43] D. Molina-Garcia, T.M. Pham, P. Paradisi, C. Manzo, and G. Pagnini. Fractional kinetics emerging from ergodicity breaking in random media. *Physical Review E*, 94:052147, 2016.

[44] A. A. Novotny and J. Sokołowski. *Topological derivatives in shape optimization*. Interaction of Mechanics and Mathematics. Springer-Verlag, Berlin, Heidelberg, 2013.

[45] A. A. Novotny, J. Sokołowski, and A. Żochowski. *Applications of the topological derivative method*. Studies in Systems, Decision and Control. Springer Nature Switzerland, 2019.

[46] M. Raberto, E. Scalas, and F. Mainardi. Waiting-times and returns in high-frequency financial data: an empirical study. *Physica A: Statistical Mechanics and its Applications*, 314(1-4):749–755, 2002.

[47] Y.A. Rossikhin and M. V. Shitikov. Application of fractional calculus for dynamic problems of solid mechanics: novel trends and recent results. *Applied Mechanics Reviews*, 63(1):010801, 2010.

[48] W. Rundell and Z. Zhang. Recovering an unknown source in a fractional diffusion problem. *Journal of Computational Physics*, 368:299 – 314, 2018.

[49] K. Sakamoto and M. Yamamoto. Initial value/boundary value problems for fractional diffusion-wave equations and applications to some inverse problems. *Journal of Mathematical Analysis and Applications*, 382(1):426–447, 2011.

[50] K. Sakamoto and M. Yamamoto. Inverse source problem with a final overdetermination for a fractional diffusion equation. *Mathematical Control & Related Fields*, 1(4):509, 2011.

[51] A. Schumacher. *Topologieoptimierung von bauteilstrukturen unter verwendung von lochpositionierungkriterien*. Ph.D. Thesis, Universität-Gesamthochschule-Siegen, Siegen - Germany, 1995.
[52] J. Sokołowski and A. Żochowski. On the topological derivative in shape optimization. *SIAM Journal on Control and Optimization*, 37(4):1251–1272, 1999.
[53] P. Tricarico. Global gravity inversion of bodies with arbitrary shape. *Geophysical Journal International*, 195(1):260–275, 2013.
[54] J.G. Wang, Y.B. Zhou, and T. Wei. Two regularization methods to identify a space-dependent source for the time-fractional diffusion equation. *Applied Numerical Mathematics*, 68:39–57, 2013.
[55] W. Wang, M. Yamamoto, and B. Han. Numerical method in reproducing kernel space for an inverse source problem for the fractional diffusion equation. *Inverse Problems*, 29(9):095009, 2013.
[56] T. Wei, X.L. Li, and Y.S. Li. An inverse time-dependent source problem for a time-fractional diffusion equation. *Inverse Problems*, 32(8):085003, 2016.
[57] T. Wei and J. Wang. A modified quasi-boundary value method for an inverse source problem of the time-fractional diffusion equation. *Applied Numerical Mathematics*, 78:95–111, 2014.
[58] T. Wei and J.G. Wang. A modified quasi-boundary value method for the backward time-fractional diffusion problem. *ESAIM: Mathematical Modelling and Numerical Analysis*, 48(2):603–621, 2014.
[59] T. Wei and Z.Q. Zhang. Reconstruction of a time-dependent source term in a time-fractional diffusion equation. *Engineering Analysis with Boundary Elements*, 37(1):23–31, 2013.
[60] A. Wexler, B. Fry, and M. R. Neuman. Impedance-computed tomography algorithm and system. *Applied optics*, 24(23):3985–3992, 1985.
[61] M. Yamamoto and Y. Zhang. Conditional stability in determining a zeroth-order coefficient in a half-order fractional diffusion equation by a carleman estimate. *Inverse problems*, 28(10):105010, 2012.
[62] S. B. Yuste, L. Acedo, and K. Lindenberg. Reaction front in an a+ b→ c reaction-subdiffusion process. *Physical Review E*, 69(3):036126, 2004.
[63] S. B. Yuste and K. Lindenberg. Subdiffusion-limited reactions. *Chemical physics*, 284(1-2):169–180, 2002.
[64] Y. Zhang, X. Liu, M.R. Belić, W. Zhong, Y. Zhang, and M. Xiao. Propagation dynamics of a light beam in a fractional Schrödinger equation. *Physical Review Letters*, 15:180403, 2015.
[65] Y. Zhang, M.M. Meerschaert, and R.M. Neupauer. Backward fractional advection dispersion model for contaminant source prediction. *Water Resources Research*, 52(4):2462–2473, 2016.
[66] Y. Zhang and X. Xu. Inverse source problem for a fractional diffusion equation. *Inverse problems*, 27(3):035010, 2011.

(R. Prakash) Departamento de Matemática, Facultad de Ciencias Físicas y Matemáticas, Universidad de Concepción, Avenida Esteban Iturra s/n, Bairro Universitario, Casilla 160 C, Concepción, Chile.
Email address: rprakash@udec.cl

(M. Hrizi) Monastir University, Department of Mathematics, Faculty of Sciences Avenue de l'Environnement 5000, Monastir, Tunisia
Email address: mourad-hrizi@hotmail.fr

(A.A. Novotny) Laboratório Nacional de Computação Científica LNCC/MCT, Coordenação de Métodos Matemáticos e Computacionais, Av. Getúlio Vargas 333, 25651-075 Petrópolis - RJ, Brasil
Email address: novotny@lncc.br